Journal of Constructional Steel Research 123 (2016) 135–143

Contents lists available at ScienceDirect

Journal of Constructional Steel Research

System-based design of planar steel frames, I: Reliability framework

Hao Zhang [a,*], Shabnam Shayan [a], Kim J.R. Rasmussen [a], Bruce R. Ellingwood [b]

[a] The University of Sydney, Australia
[b] Colorado State University, United States

ARTICLE INFO

Article history:
Received 11 February 2016
Received in revised form 9 May 2016
Accepted 9 May 2016
Available online 17 May 2016

Keywords:
Buildings (codes)
Advanced analysis
Inelastic analysis
Structural reliability
Steel structure
Structural engineering
Nonlinear frame analysis
Probability-based design

ABSTRACT

The design of steel frames by advanced analysis (second-order inelastic analysis with imperfections) of overall system behaviour is permitted in the American steel specification AISC360-10 and the Australian Standard AS4100. In both specifications, the strength of a structural frame can be determined by a rigorous system nonlinear analysis in lieu of checking member resistances to the specific provisions of the Specification, provided that the limit states covered by the Specification equations are detected by the inelastic analysis, and a comparable or higher level of structural reliability is achieved by the inelastic analysis than by member-based design. This system-based, design-by-advanced analysis approach is termed "Direct Design Method" (DDM). In DDM, a system resistance factor is applied to the frame strength. The system factor in AISC360-10 was adopted without considering its impact on frame reliability. This paper describes the framework for developing reliability-based system resistance factors suitable for use with DDM. A simple frame is used to demonstrate the procedures. Appropriate system resistance factors for various load cases and design recommendations are presented in a companion paper [1] based on the system reliability analyses of a series of steel frames.

1. Introduction

In conventional steel design methods, structural members and connections are designed individually based on component strength limit states. Structural system effects are reflected in the current steel designs, but only implicitly through the use of effective length factors and similar approximations. The design customarily has been based on elastic analysis. This component-based, elastic approach cannot accurately predict the complex interactions between members of a large structural system, nor can it capture the inelastic load redistribution subsequent to first yielding. The load-carrying capacity of a structural steel system with even a modest capacity to redistribute loads can be larger than what is determined by the design of individual members [2–8]. Therefore, there are strong reasons for designing a steel frame as a whole system rather than an assembly of individual components, particularly with the advent of performance-based design in modern engineering practice.

Recent advances in nonlinear structural modelling make it possible to address the issue of designing a steel frame as a system rather than as a set of independent components [2,9–17]. Many studies have demonstrated that the ultimate limit state strength and stability of a real steel structure system can be most accurately captured by the geometric and material nonlinear analysis with imperfections. Analysis with this capability is termed "advanced analysis" in the Australian Steel Structures Standard AS4100 Appendix D [18], and termed "inelastic analysis" in the American Institute of Steel Construction Specification AISC360-10 Appendix 1 [19]. The advantages of the *design-by-analysis* approach are evident in several aspects. For one, the system strength can be directly evaluated from analysis without the need for checking member and connection resistances to the specific provisions. Also, advanced analysis may lead to the design of lighter and more economic structures. For example, Ziemian, et al. [20] analysed a series of two-bay two-storey planar frames and a 22-storey 3D frame. It was shown that design by advanced analysis could save about 12% of steel weight compared to traditional design by the AISC Load and Resistance Factor Design (LRFD) method. More importantly, with advanced analysis, engineers are better able to understand the system behaviours. This system-based, design-by-advanced analysis approach is termed "Direct Design Method" (DDM) in the present study. The change of emphasis from individual member strengths to the overall structural behaviour will promote a more holistic approach and greater innovations in structural design. It should be noted that the Direct Design Method is different from the "Direct Analysis Method" (abbreviated as "DM" in the AISC Specification), stipulated in Section C1.1 of AISC360-10 [19]. DM is based on a rigorous second-order analysis directly modelling member imperfections. In the DM, member and system instability are checked/detected by the analysis, the equation based design checks only need to be completed at the cross section level. While DM eliminates the need for calculating effective length factor, it is still a member-based design approach as

* Corresponding author.
E-mail addresses: hao.zhang@sydney.edu.au (H. Zhang), shabnam.shayan@sydney.edu.au (S. Shayan), kim.rasmussen@sydney.edu.au (K.J.R. Rasmussen), bre@engr.colostate.edu (B.R. Ellingwood).

http://dx.doi.org/10.1016/j.jcsr.2016.05.004
0143-974X/

opposed to system checks. The "Direct Design Method" (DDM) presented in this paper is a system-based approach, which is similar to the design procedure stipulated in Appendix 1 – Inelastic Analysis and Design – of AISC360-10 and is an extension of the DM. Therefore, the two methods are different.

The AISC Specification 360–10 permits design through inelastic analysis of overall system behaviour (except for seismic design), provided that (1) the limit states covered by the Specification equations are detected by the inelastic analysis; (2) members and connections with elements subject to yielding have adequate ductility; and (3) a comparable or higher level of structural reliability is provided by the inelastic analysis than by member-based design. The ad hoc AISC approach to ensure structural reliability in DDM is to reduce the strength and stiffness of all members and connections by a factor of 0.9. The AISC360 commentary acknowledges that this factor of 0.90 has its origin in the AISC LRFD resistance factors of tension and flexural members that yield; its use in system-based design, although "deemed acceptable", is not based on any system reliability analysis. There is a lack of research to develop the system resistance factors based on rigorous system reliability considerations.

Consistent with the LRFD philosophy, if advanced analysis is used to determine the ultimate strength of a structural system, an appropriate system resistance factor (ϕ_s) which accounts for the main factors influencing the reliability of a frame must be provided. The resistance factor is applied to the entire system strength, rather than to each component, to account for potential risks arising from uncertainties. The development of system resistance factors requires rigorous system reliability analyses.

This paper outlines a framework of developing the system resistance factors for DDM. A sample planar frame is used to demonstrate the procedures of assessing system reliability and developing the system resistance factors. The companion paper [1] examines an extensive range of planar low-to-mid-rise moment resisting and braced frames with regular and irregular configurations, with the aim of providing suitable system resistance factors to be used for system-based design.

2. Direct design method

Consistent with the current LRFD philosophy, in DDM a global system resistance factor is applied to the nominal frame strength. Thus the familiar LRFD format can be applied in an integral sense for the whole frame:

$$\phi_s R_n \geq \sum \gamma_i Q_{ni} \tag{1}$$

in which R_n represents the nominal system strength determined by advanced analysis with nominal (unreduced) values of structural properties (i.e., strength, stiffness, dimension), ϕ_s is a system resistance factor, Q_{ni} are the nominal loads (i.e., D_n, L_n and W_n for dead, live and wind loads, respectively), and γ_i is the load factor for Q_{ni}. The subscript "n" in Eq. (1) emphasizes that those terms are code-specified nominal values used in design.

In conducting a nonlinear structural analysis, the loads are increased incrementally by using a load scale factor λ. The loads are scaled up until failure of the frame occurred to determine the ultimate load scale factor λ_u. The ultimate strength of a frame is defined as the peak load in the frame's load–displacement response (at a certain key location). If the load–displacement response does not have a descending branch, it is assumed that the ultimate strength is reached when the slope of the load–displacement curve reduces to 5% of its initial value. Eq. (1) can be rewritten as

$$\lambda_u \geq \frac{1}{\phi_s} \tag{2}$$

in which λ_u represents the ultimate load scale factor under the applied loads $\sum \gamma_i Q_{ni}$. It is assumed for code implementation purposes that the current load combination rules (for member-based design) are still applicable to checking overall system response. Thus, the load factors γ_i are taken from the existing load standard. The value of system resistance factor will be determined using structural reliability theory to assure a (pre-defined) target level of structural reliability.

2.1. System reliability analysis

The structural system probability of failure, denoted by P_f, is given by:

$$P_f = \mathrm{P_r}(R-Q \leq 0) = \mathrm{P_r}[g(R,Q) \leq 0] = \int \ldots \int_{g(X)\leq 0} f_{\boldsymbol{x}}(\boldsymbol{x}) d\boldsymbol{x} \tag{3}$$

in which $\mathrm{P_r}(\,)$ represents the probability of the event in the bracket, R is the system resistance, Q represents the applied load(s), and $g(\,)$ is the limit state function defined such that $g(\,) \leq 0$ defines the unsafe (failure) domain. $\mathbf{X} = (X_1, \ldots . X_n)$ is an n-dimensional vector of basic random variables representing uncertainties such as material strength, stiffness and applied load. $f_{\mathrm{x}}(\mathrm{x})$ is the joint probability density function (PDF) for $\mathbf{X}$. Note that R and Q are functions of $\mathbf{X}$. In practice, P_f is often converted to a reliability index, β, which serves as an alternative and more familiar measure of reliability [21]. The reliability index is related to P_f by $\beta = \Phi^{-1}(1-P_f)$, in which Φ represents the standard normal distribution function (zero mean and unit variance), and Φ^{-1} is the inverse function of Φ.

Considering the load criteria in ASCE7-5 [22], if a frame as a system is at its limit under gravity loads, then the design equation of Eq. (1) becomes

$$\phi_s R_n = 1.2D_n + 1.6L_n \tag{4}$$

and the limit state function g is given by

$$g = R_G - D - L \tag{5}$$

in which R_G represents the system's gravity resistance, D is the dead load, and L represents the (lifetime maximum) live load. Note that R_G, D and L are random variables, while R_n, D_n and L_n are nominal values.

For a frame at its strength limit under combined gravity and wind loads, the design equation is

$$\phi_s R_n = 1.2D_n + 0.5L_n + 1.6W_n. \tag{6}$$

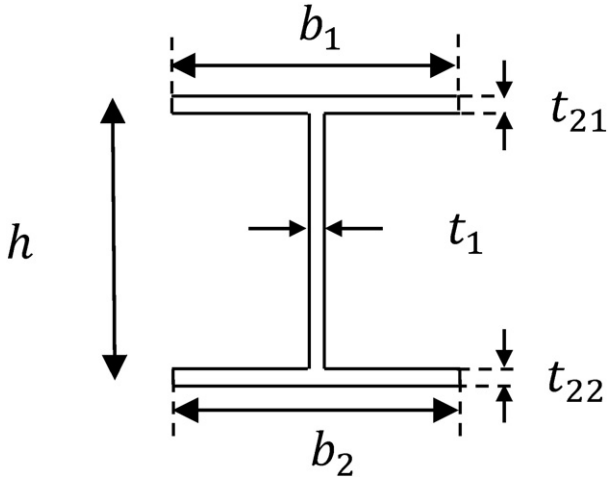

Fig. 1. Cross-section dimensions.

Table 1
Statistical results for cross-section dimensions [25].

Thickness	Mean/Nominal	COV
Section depth (h)	1.001	0.0044
Section width (b_1)	1.012	0.01
Section width (b_2)	1.015	0.0095
Web thickness (t_1)	1.055	0.04
Flange thickness (t_{21})	0.988	0.044
Flange thickness (t_{22})	0.988	0.049

Note that Eq. (6) represents the dead load plus "arbitrary point-in-time" live load (L_{apt}) and the (lifetime maximum) wind load. For this load combination, we are concerned about the system's lateral load capacity, and the governing system limit state can be expressed as

$$g = R_w - W \tag{7}$$

in which W is the wind load, and R_w denotes system's lateral load capacity under the applied dead load and the "arbitrary-point-in-time" live load. W and R_w are expressed in dimensionally consistent units.

One way to compute the probability of failures for Eqs. (5) and (7) is to use the direct Monte Carlo simulation in which random variables are sampled randomly and repeatedly to observe the result. The probability of failure is estimated by

$$P_f \cong \frac{n}{N} \tag{8}$$

in which N is the total number of simulations, and n denotes the number of simulation for which the system failed. For typical structural reliability assessments (i.e., P_f on the order of 10^{-3}), such a direct simulation method requires a large number of N to sufficiently capture the lower tail behaviour of the distribution of structural strength. Obviously the computing burden of the direct Monte Carlo simulation is very high as it requires performing N advanced analyses.

In this study, the probability of failure is estimated using a simplified method following the concept of First-Order Reliability Method (FORM) [21]. In this method, the probabilistic models (distribution type and distribution parameters) of system resistance (R_G and R_w) are estimated first using simulation taking into account the uncertainties in material stiffness and strength, and subsequently are combined with the load distributions using the FORM. In this simplified method, relatively few simulations (e.g., 300 to 500 simulations) are sufficient for estimating the cumulative distribution function (CDF) of system resistance R [21]. The efficiency of sampling can be further improved by using the Latin Hypercube sampling (LHS) technique. The probabilistic models of loads are available from the literature as described subsequently. Once the statistics of system strength and loads are known, the probability failures for Eqs. (5) and (7) can be readily computed using the FORM.

2.2. Procedures for developing ϕ_s for DDM

The procedure for developing system resistance factors suitable for use with DDM can be summarized in the following steps:

(1) A suite of low-to-mid-rise steel frames are selected to represent the current steel building inventory and cover all ranges of system behaviours, including different failure modes (elastic/inelastic failure, strong column-weak beam and weak column-strong beam framing systems, redundancy, ductility, regular/irregular structural configurations, connection type, etc.). The frames are subjected to gravity loads, and combined gravity and wind loads.
(2) A range of ϕ_s values are considered for each frame. For a given ϕ_s, the designs of the frames are adjusted such that the frames are just at their strength limit.
(3) Probabilistic assessments of the strengths of all frames are conducted using Monte Carlo simulation combined with advanced analysis to generate distributions of the system resistance, taking into account the randomness in material and geometric properties.
(4) Using the statistics for the system resistance obtained in Step 3, and the probabilistic models of the loads, the reliability index β of each frame is computed.
(5) Steps 3 and 4 are repeated to obtain the relationships between β and ϕ_s. The results can then be used by the specification writing group to choose resistance factors corresponding to desired reliabilities.

Table 2
Correlation matrix for cross-section dimensions [25].

	h	b_1	b_2	t_1	t_{21}	t_{22}
h	1	−0.0068	0.0534	0.0399	−0.0686	−0.0989
b_1	−0.0068	1	0.6227	−0.2142	−0.2681	−0.1456
b_2	0.0534	0.6227	1	−0.2132	−0.1596	−0.0423
t_1	0.0399	−0.2142	−0.2132	1	0.2368	0.2451
t_{21}	0.0686	−0.2681	−0.1596	0.2368	1	0.7634
t_{22}	0.0989	−0.1456	0.0423	0.2451	0.7634	1

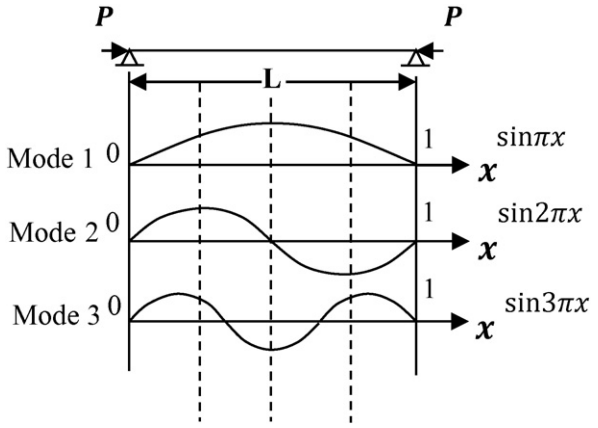

Fig. 2. First three buckling modes of a simply supported axially loaded column.

Steps 2–5 will be demonstrated using a simple planar moment frame in this paper.

3. Uncertainties in steel frame systems

This section summarizes the probabilistic models for the basic random variables considered in this study, including yield stress, elastic modulus, residual stress, cross-sectional dimensions, member out-of-straightness, frame out-of-plumbness, and structural loads.

3.1. Variability in yield stress and elastic modulus

Yield stress often has a significant influence on the load-carrying capacity of a frame system. Yield stress is modeled by a lognormal distribution with a mean-to-nominal value of 1.05 and a coefficient of variation (COV) of 0.1 [23]. Note that these statistics are based on tests of steels that were manufactured in the 1970′s. Recent studies of steel

Table 3
Statistics for out-of-straightness scale factors [28].

Statistics	a_1/L	a_2/L	a_3/L
Mean	0.000556	0.000139	0.000073
Standard deviation	0.000427	0.000071	0.000078
Distribution	Normal	Normal	Normal

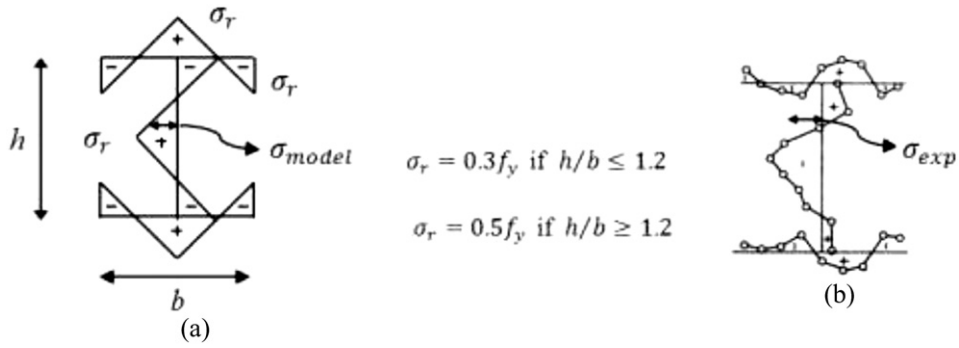

Fig. 3. Residual stress: (a) ECCS pattern; and (b) typical actual measurement.

properties for modern grades of steel have indicated that the mean-to-nominal ratio and COV both are somewhat less due to better controlled manufacturing processes [24]. However, it has been found that these differences in statistics do not have a significant impact on the reliabilities presented herein. The modulus of elasticity is modeled as a normally distributed random variable with a mean equal to the nominal value and a COV of 0.06 [23].

3.2. Variability in cross-section dimensions

Steel section properties were statistically examined in [25] based on the measurements of 369 hot-rolled I-sections. The statistical data for the cross-section dimensions shown in Fig. 1 are listed in Table 1. Correlations observed between section parameters are summarized in Table 2.

Using the statistics in Tables 1 and 2, it was found that both the moment of inertia and cross-sectional area have a mean-to-nominal ratio of unity and a COV of about 0.05; these results are comparable to those reported elsewhere [26,27].

3.3. Variability in initial geometric imperfections

The member initial out-of-straightness can be expressed as the combination of a given number of buckling modes of a single column under compression [28]:

$$\delta = \sum_{i=1}^{m} a_i \sin(i\pi x) \tag{9}$$

in which $x \in [0,1]$ is the normalized coordinate along the length of the member, δ denotes the initial out-of-straightness at location x, a_i is the scale factor for the ith mode, and is modeled as a random variable. It has been shown that in general, using the first 3 modes is sufficient to model member out-of-straightness [28]. To determine the statistics for the scale factors a_i, the initial-out-straightness data of hot-rolled IPE-160 columns reported by ECCS Committee 8.1 [29] were analysed. The reported data comprise the out-of-straightness measured at mid-length and quarter points. The measured imperfections were extracted into first three buckling modes (Fig. 2). The mean and COV of the three scale factors were determined and summarized in Table 3. Details can be found elsewhere [28]. Using the statistics shown in Table 3a random member imperfection can be simulated by generating a random scale factor and a random sign for each mode and then combining the three modes.

The frame out-of-plumb is treated as a random variable and modeled as all columns leaning in the same direction. The statistics for frame out-of-plumb has been studied in [28], and it was found that the out-of-plumb angle can be modeled as a lognormal distribution, with a mean of approximately 1/770 and a standard deviation of 1/880.

3.4. Variability in residual stress

This study considers the variability in the magnitude of residual stress. The pattern of residual stress is assumed to be deterministic, following the "ECCS" (European Council for Constructional Steelworks) residual stress pattern shown in Fig. 3. To model the uncertainty in the magnitude of residual stress, a random scale factor x is applied to the ECCS residual stress pattern. A total of 63 actual residual stress measurements from the literature were used to determine the statistics of the scale factor [30]. For a given residual stress measurement, the scale factor is obtained by minimizing the error between the actual residual stress and the (scaled) ECCS result:

$$\text{Error} = \sum_{i=1}^{n} \left(x\sigma_m^i - \sigma_e^i \right)^2 \tag{10}$$

in which n = total number of measured nodes, i = ith node, x = scale factor, σ_m^i = the scaled, theoretical value at node i, σ_e^i = measured

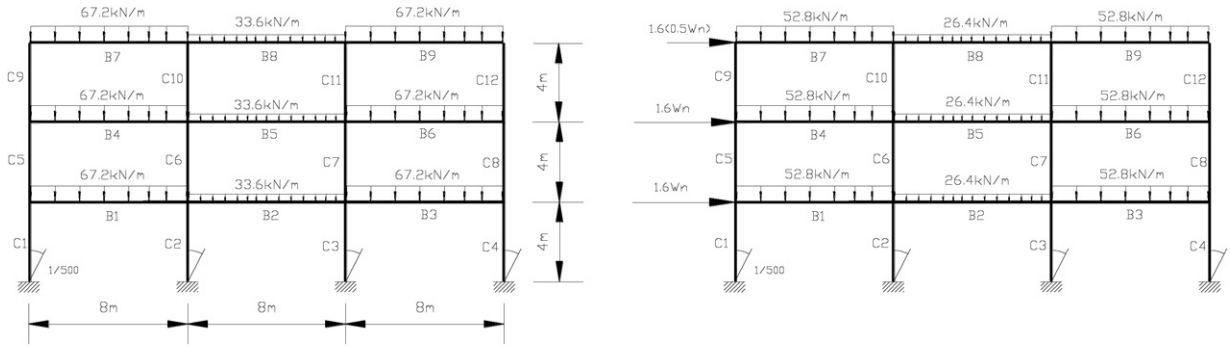

Fig. 4. A three-bay three-storey frame, (a) gravity load; and (b) combined gravity and wind loads.

Table 4
System based design under gravity load only.

Members	$\phi_s = 0.63$	$\phi_s = 0.69$	$\phi_s = 0.74$	$\phi_s = 0.86$	$\phi_s = 0.96$
	Sections	Sections	Sections	Sections	Sections
C1,C4,C5,C8,C9,C12	250UC72.9	250UC72.9	200UC59.5	250UC72.9	250UC72.9
C2,C3,C6,C7	200UC59.5	200UC59.5	200UC59.5	200UC59.5	200UC59.5
C10,C11	150UC30.0	150UC30.0	150UC30.0	150UC30.0	150UC30.0
B1,B3,B4,B6,B7,B9	460UB74.6	460UB67.1	460UB67.1	360UB56.7	360UB50.7
B2,B5,B8	360UB56.7	360UB50.7	360UB50.7	360UB50.7	310UB46.2

value at node *i*. This error minimization process was conducted for all 63 samples. It was found that the scale factor *x* has a mean of 1.047 with a COV of 0.21, and can be best fitted by a normal distribution [30].

3.5. Variability in structural loads

The statistics of loads can be obtained from the literature [31]. The present study uses the load criteria appearing in ASCE7–05. The dead load is assumed to be normally distributed with a mean-to-nominal value of 1.05 and a COV of 0.1. The (lifetime maximum) live load is modeled by an Extreme Type I distribution with a mean-to-nominal value of 1.0 and a COV of 0.25. The "arbitrary-point-in time" live load has a Gamma distribution with a mean of $0.24L_n$ and a COV of 0.6. The wind load is modeled by an Extreme Type I distribution with a mean of $0.92W_n$ and a COV of 0.37.

4. Example frame

A three-bay, three-storey planar steel frame has been selected as an example to demonstrate the procedure for developing the system resistance factor. Fig. 4 shows the geometry of the frame. The nominal yield strength f_y and modulus of elasticity E are 320 MPa and 200 GPa, respectively. The stress–strain relation of the steel was initially described by a tri-linear curve, consisting of an elastic part and a yield plateau extending to a strain of $10\varepsilon_y$ followed by a strain-hardening part with a strain-hardening modulus of $E_{sh} = 0.02E$, where $\varepsilon_y = f_y/E$ is the yield strain. However, it was found that the strain hardening has an insignificant effect for the ultimate strengths of the frames considered in this study [32]. Hence, the steel is modeled as elastic-perfectly-plastic in this study. A nominal frame out-of-plumbness of 1/500 (which is the maximum out-of-plumbness specified by AISC) is assumed in the design. The residual stress was modeled as a self-equilibrating initial stress following the ECCS residual stress pattern. All beams and columns are compact and laterally braced so that local buckling and lateral-torsional buckling are not considered. Connections are assumed to be fully rigid; compliance of the connections is not considered. Furthermore, it is assumed that the connections have sufficient ductility and are capable of maintaining their design strength while accommodating inelastic deformation demands.

The second-order inelastic finite element (FE) models were developed using the software OpenSEES [33], accounting for all material and geometrical nonlinearities. Displacement-based, fibre-type beam elements were used to trace the spread of plasticity through the cross-section and along the members. Typically, each column/beam was discretised into twenty elements. Frame out-of-plumbness was modeled by the notional load approach. Arc-length techniques were used to obtain the complete load-deflection response at key locations (e.g. load versus roof drift).

Two load criteria from ASCE7-05 were considered, i.e., $1.2D_n + 1.6L_n$ and $1.2D_n + 0.5L_n + 1.6W_n$. In ASCE7-05, the design wind load, $1.6W_n$, is based on a wind speed with a return period of 50 years (V_{50}). In the more recent standard ASCE7-10, the design wind load, $1.0W_n$, is based on a wind speed with a return period of 700 years (V_{700}) for the structures of Risk Category II. In the upcoming standard ASCE7-16, the design wind load, $1.0W_n$, is also based on a wind speed with a return period of 700 years. Since the ratio $V_{700}/V_{50} \approx \sqrt{1.6}$, the design wind loads are approximately the same in all three standards. Hence the system resistance factors developed in this work is also applicable to ASCE7-10 and upcoming ASCE7-16.

Because dead load, live load and wind load all have different variabilities, the reliability studies need to consider various loading conditions. In the case of gravity loads, the typical factored gravity load is $1.2D_n + 1.6L_n = 67.2$ kN/m as shown in Fig. 4, with L_n/D_n varying from 0.5 to 5.0. For instance, for $L_n/D_n = 2$, $L_n = 30.55$ kN/m, and $D_n = 15.27$ kN/m. For the combined wind and gravity load case, L_n and D_n are assumed to be 48 kN/m and 24 kN/m, respectively; the nominal wind load W_n varies from 86.4 kN to 277.2 kN to consider different lateral-to-gravity load ratios. Let W_T and G_T denote the overall factored wind force and the overall factored gravity force on the building,

$$W_T = \Sigma_i 1.6W_{ni}, G_T = \Sigma_i (1.2D_{ni} + 0.5L_{ni})A_i$$

in which W_{ni}, D_{ni}, L_{ni} and A_i represent the wind force, dead load, live load and floor area at level *i*, respectively. Four cases of the wind-to-gravity force ratio W_T/G_T are considered in this study, i.e., $W_T/G_T = 0.11$, 0.15, 0.25 and 0.35.

4.1. System reliability analysis-gravity load only

To consider the effect on system reliability of ϕ_s, the design of the frame is adjusted such that the frame is at its strength limit state under a given value of ϕ_s. Table 4 summarizes five values of ϕ_s and the

Table 5
Simulation results for system's gravity load capacity.

ϕ_s	μ_R (kN/m)	V_R
0.63	80.06	0.08
0.69	72.86	0.08
0.74	68.32	0.08
0.86	58.30	0.08
0.96	52.31	0.09

μ_R = mean; V_R = COV

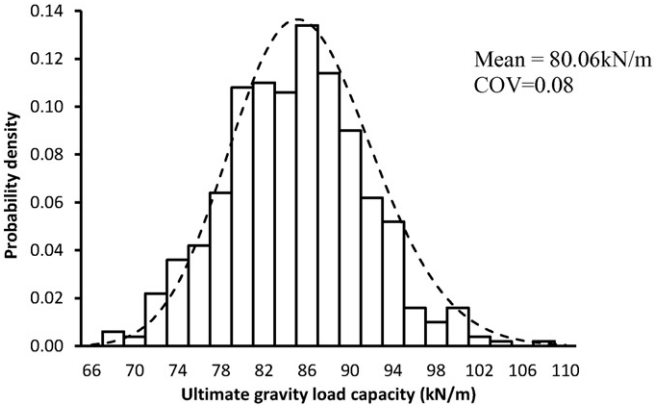

Fig. 5. Histogram of gravity load capacity, ($\phi_s = 0.63$).

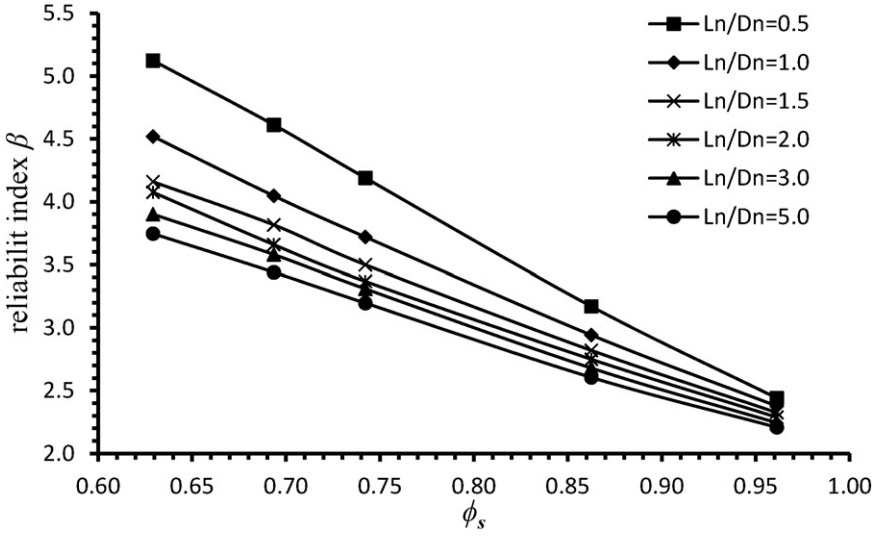

Fig. 6. β vs. ϕ_s, gravity load only.

corresponding member sizes. Take the case of $\phi_s = 0.63$ as an example, the ultimate load scale factor λ_u is 1.59 so that with a system resistance factor $\phi_s = 0.63$, the frame is just at its strength limit state ($\lambda_u \phi_s = 1.0$). The frame member sizes were then adjusted such that the frame is at its strength limit state for other values of ϕ_s as well.

Monte Carlo simulation using Latin Hypercube sampling technique were conducted to generate sample distributions of the system strength, based on which we can estimate its statistics. 350 simulations were performed for each frame. In each simulation, a sample of frame is generated with randomly generated values for yield strength, modulus of elasticity, initial geometric imperfections, and residual stress, according to their statistics presented in Section 3. Assuming that the loads at every level are perfectly correlated, the frame is loaded with an increasing gravity load until collapse to obtain the ultimate gravity load capacity R_G. Based on the Monte Carlo simulation, the statistics of R_G (mean and COV) for different values of ϕ_s are summarized in Table 5. It can be seen that the mean of R_G decreases as ϕ_s increases. This is to be expected as a smaller value of ϕ_s represents a more conservative design. Table 5 also shows that the COV of R_G appears to be independent with ϕ_s; it is about 8% in all cases. A lognormal distribution can fit to the histogram of R_G. This is consistent with the common observation that structural resistance often can be modeled by a lognormal distribution. As an example, Fig. 5 shows the histogram of R_G for the frame assigned with $\phi_s = 0.63$.

With known statistics of R_G (from simulation) and the loads (from literature), the reliability index for Eq. (5) can be computed using the FORM procedure outlined in Section 2.1. Fig. 6 plots the system reliability indices β as a function of ϕ_s for different cases of L_n/D_n. It

Table 6
System resistance factors (ϕ_s) for different reliability levels, gravity load only.

L_n/D_n	Weight (%)	ϕ_s			
		$\beta = 2.5$	$\beta = 2.75$	$\beta = 3.0$	$\beta = 3.5$
0.5	10	0.95	0.92	0.89	0.82
1	20	0.94	0.89	0.85	0.78
1.5	25	0.93	0.88	0.83	0.74
2	35	0.92	0.86	0.81	0.72
3	7	0.90	0.85	0.80	0.71
5	3	0.89	0.83	0.78	0.68
		0.92	0.87	0.83	0.74
Average weighted value of ϕ_s					

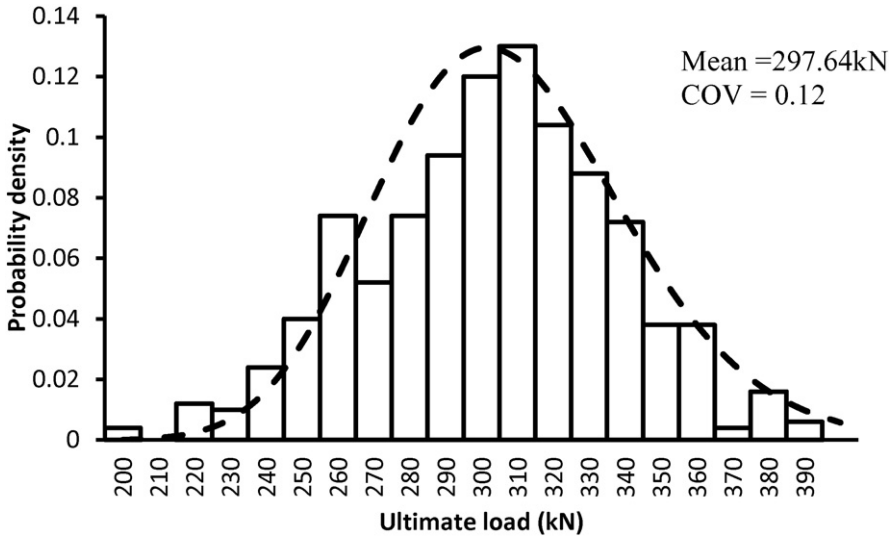

Fig. 7. Histogram of R_W, ($W_T/G_T = 0.15$, $\phi_s = 0.87$).

Table 7
Simulation results for system's lateral load capacity.

$W_T/G_T = 0.11$			$W_T/G_T = 0.15$			$W_T/G_T = 0.25$			$W_T/G_T = 0.35$		
ϕ_s	μ_R (kN)	V_R	ϕ_s	μ_R (kN)	V_R	ϕ_s	μ_R (kN)	V_R	ϕ_s	μ_R (kN)	V_R
0.75	289.15	0.13	0.76	350.96	0.12	0.74	535.92	0.10	0.75	684.20	0.08
0.83	243.00	0.13	0.80	331.42	0.12	0.80	499.84	0.11	0.79	638.77	0.09
0.88	225.01	0.14	0.87	297.64	0.12	0.86	449.72	0.10	0.87	582.89	0.10
0.93	208.95	0.15	0.93	268.22	0.13	0.95	391.81	0.11	0.95	523.05	0.09

μ_R = mean; V_R = COV.

can be seen that for a given value of ϕ_s, β decreases as L_n/D_n increases. This is because live load has more variability than dead load. The results of Fig. 6 can be used to select a required ϕ_s in order to achieve a given value of target reliability index. Table 6 summarizes the ϕ_s values for four representative target reliability index (i.e. $\beta = 2.5$, 2.75, 3 and 3.5) for different live-to-dead load ratios. Clearly, a single value of ϕ_s cannot achieve a "uniform" reliability. However, a constant resistance factor for all load ratios is desirable for its simplicity in everyday design use. To obtain a weighted average value of ϕ_s, a weight is assigned to each case of L_n/D_n, representing the relative frequency of different load situations [34]. These weights reflect the best judgement of the authors. Thus, the final system resistance factor ϕ_s can be calculated as

$$\phi_s = \sum w_i \phi_{si}$$

in which w_i is the weight assigned to the ith load situation, and ϕ_{si} is the system resistance factor for the ith load situation. Table 6 summarizes the weight-averaged resistance factors for different target reliability indices.

4.2. System reliability analysis – combined gravity and wind loads

For a given combination of ϕ_s and wind-to-gravity load ratio W_T/G_T, the member section sizes are adjusted such that the frame is just at its strength limit state. The section sizes for different combinations of W_T/G_T and ϕ_s can be found in the Appendix A.

For each design of the frame, 350 Monte Carlo simulations were performed to obtain a sample of its lateral capacity. In each simulation, a random frame is generated, and subjected to a random dead load and a random arbitrary-point-in-time live load. Loads on each level are assumed to be perfectly correlated. The frame is analysed under the applied gravity loads. Once the deformed shape of the frame under gravity loading is obtained and the gravity loads are in position, a static lateral pushover analysis is conducted by increasing the lateral load until failure. The applied lateral load at system failure represents the lateral load capacity of the system, R_W. Fig. 7 shows the histogram of R_W for the frame with $W_T/G_T = 0.15$ and $\phi_s = 0.87$. The statistics of R_W for different combinations of W_T/G_T and ϕ_s are summarized in Table 7. Similar to the gravity load case, the mean of R_W decreases with increasing ϕ_s. However, its COV appears to be independent of ϕ_s; it is about 10% to 15% in all cases. It is also found that in general, R_W can be fitted by a log-normal distribution.

The reliability indices for all cases were computed using the FORM outlined in Section 2.1, and summarized in Table 8. To verify the accuracy of the FORM, the results from the direct Monte Carlo simulations are also presented in Table 8. As can be seen from Table 8, the reliability indices from the FORM are generally slightly lower than those from the Monte Carlo simulations. The discrepancy of β is about 2% to 5%. This shows that the simplified FORM is reasonably accurate, and sufficient for code development purpose. The following discussions are based on the results from the FORM.

The system reliability indices for all combinations of ϕ_s and W_T/G_T are plotted in Fig. 8. It is evident that β decreases as W_T/G_T increases. This is to be expected because the COV of the wind load is greater than that of the gravity loads. It can be seen from Fig. 8 that for $\phi_s = 0.85$, β approaches a value of 2.5 when the wind is the major load component; with greater gravity loads, the value of β increases to about 3.1. By assigning weights to different wind-to-gravity load ratio W_T/G_T, the weighted-average values of system resistance factors for different reliability levels are determined and summarized in Table 9.

Table 8
Comparison of reliability indices from FORM and direct MC simulations.

W_T/G_T	ϕ_s	β (FORM)	β (MC)	Error
0.11	0.75	3.55	3.62	1.86%
	0.83	3.09	3.16	2.18%
	0.88	2.85	2.94	2.95%
	0.93	2.63	2.69	2.32%
0.15	0.76	3.26	3.39	3.77%
	0.80	3.10	3.18	2.60%
	0.87	2.79	2.87	2.99%
	0.93	2.50	2.60	3.78%
0.25	0.74	3.08	3.14	1.89%
	0.80	2.78	2.86	2.79%
	0.86	2.59	2.70	4.01%
	0.95	2.25	2.33	3.27%
0.35	0.75	2.85	2.95	3.45%
	0.79	2.65	2.73	2.94%
	0.87	2.38	2.51	4.89%
	0.95	2.09	2.15	2.88%

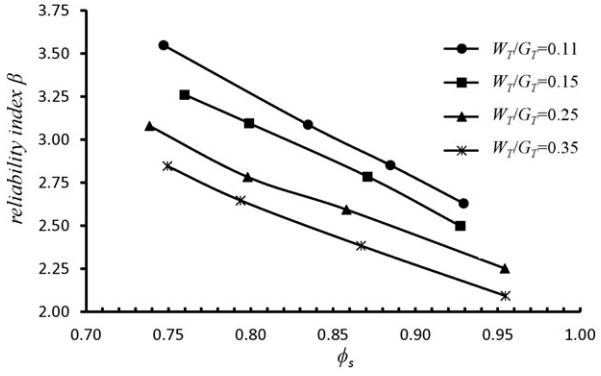

Fig. 8. β vs. ϕ_s, combined gravity and wind loads.

Table 9
System resistance factor (ϕ_s) for different reliability levels (combined gravity and wind loads).

W_T/G_T	Weight (%)	ϕ_s		
		$\beta = 2.5$	$\beta = 2.75$	$\beta = 3.0$
0.11	20	0.95	0.91	0.85
0.15	30	0.92	0.88	0.82
0.25	30	0.88	0.81	0.75
0.35	20	0.83	0.77	0.71
Final value of ϕ_s		0.90	0.84	0.78

Comparing Tables 6 and 9, it can be seen that for a particular value of resistance factor, the reliability index for wind load is somewhat lower than that for gravity load only. For instance, with $\phi_s = 0.85$, the average-weighted β is 2.9 for gravity load only, and 2.7 for combined wind and gravity loads.

5. Conclusion

This paper presents a framework for determining system resistance factors for the Direct Design Method (DDM) of steel frames by advanced analysis (second-order inelastic analysis). The system reliability analysis method is based on the concept of First-Order Reliability Method. The statistics of system strength is estimated using Monte Carlo simulations, and then compared with the structural loads to compute the system reliability indices.

As an example, a 2D three-bay, three-storey moment resisting frame is studied in this paper. The relationships between the system resistance factor ϕ_s and the system reliability index β are computed for the gravity load case and combined wind and gravity loads. Based on the system reliability analysis results, the required resistance factor ϕ_s can be determined to achieve a certain reliability level. The accuracy of the proposed simplified reliability analysis method based on FORM is verified against the direct Monte Carlo simulations and good agreement is observed. It was found that for gravity load only, a system resistance factor of $\phi_s = 0.85$ can achieve a target system reliability index of about 2.9. For combined wind and gravity load cases, a system resistance factor of $\phi_s = 0.85$ would yield a system reliability index of 2.7. Additional frame reliability analyses, system resistance factors and design recommendations for a wide range of two-dimensional frames are presented in the companion paper [1].

Acknowledgments

This research is supported by the Australian Research Council under Discovery Project Grant DP110104263. This support is gratefully acknowledged. However, any opinions and findings expressed herein are solely those of the authors, and may not necessarily reflect the positions of the sponsoring organization.

Appendix A. Frame section sizes for combined gravity and wind loads

Table A1
System based design under combined gravity and wind loading ($W_T/G_T = 0.11$).

Members	$\phi_s = 0.75$	$\phi_s = 0.83$	$\phi_s = 0.93$	Members	$\phi_s = 0.88$
	Sections	Sections	Sections	Sections	Sections
C1,C4,C5,C8,C9,C12	460UB74.6	460UB67.1	360UB56.7	C1,C4	460UB67.1
C2,C3,C6,C7	360UB50.7	310UB46.2	360UB50.7	C5,C8,C9,C12	360UB56.7
C10,C11	250UB31.4	250UB25.7	250UB25.7	C2,C3,C6,C7	310UB40.4
B1,B3,B4,B6,B7,B9	460UB74.6	460UB74.6	460UB67.1	C10,C11	250UB25.7
B2,B5,B8	360UB56.7	360UB56.7	360UB50.7	B1,B3,B4,B6,B7,B9	460UB82.1
				B2,B5,B8	360UB56.7

Table A2
System based design under combined gravity and wind loading ($W_T/G_T = 0.15$).

Members	$\phi_s = 0.76$	$\phi_s = 0.80$	$\phi_s = 0.93$	Members	$\phi_s = 0.87$
	Sections	Sections	Sections	Sections	Sections
C1,C4,C5,C8,C9,C12	460UB67.1	460UB74.6	460UB67.1	C1,C4	460UB67.1
C2,C3,C6,C7	460UB67.1	410UB67.1	360UB50.7	C5,C8,C9,C12	360UB50.7
C10,C11	250UB37.3	250UB31.4	250UB31.4	C2,C3,C6,C7	410UB59.7
B1,B3,B4,B6,B7,B9	460UB82.1	460UB74.6	460UB74.6	C10,C11	250UB31.4
B2,B5,B8	360UB56.7	360UB56.7	360UB56.7	B1,B3,B4,B6,B7,B9	460UB67.1
				B2,B5,B8	360UB50.7

Table A3
System based design under combined gravity and wind loading ($W_T/G_T = 0.25$).

Members	$\phi_s = 0.76$	$\phi_s = 0.80$	$\phi_s = 0.86$	$\phi_s = 0.95$
	Sections	Sections	Sections	Sections
C1,C4,C5,C8,C9,C12	530UB92.4	530UB82.0	530UB82.0	460UB74.6
C2,C3,C6,C7	530UB82.0	460UB82.1	460UB82.1	460UB74.6
C10,C11	310UB46.2	310UB46.2	310UB46.2	310UB46.2
B1,B3,B4,B6,B7,B9	530UB82.0	530UB92.4	460UB74.6	460UB74.6
B2,B5,B8	460UB67.1	460UB67.1	410UB53.7	410UB53.7

Table A4
System based design under combined gravity and wind loading ($W_T/G_T = 0.35$).

Members	$\phi_s = 0.75$	$\phi_s = 0.79$	$\phi_s = 0.87$	$\phi_s = 0.95$
	Sections	Sections	Sections	Sections
C1,C4,C5,C8,C9,C12	610UB101	530UB92.4	530UB92.4	530UB92.4
C2,C3,C6,C7	610UB101	610UB101	530UB92.4	530UB82.0
C10,C11	310UB46.2	310UB46.2	310UB46.2	310UB46.2
B1,B3,B4,B6,B7,B9	530UB92.4	530UB92.4	530UB92.4	460UB82.1
B2,B5,B8	460UB67.1	460UB67.1	460UB67.1	460UB67.1

References

[1] H. Zhang, S. Shayan, K.J.R. Rasmussen, B.R. Ellingwood, System-based design of planar steel frames, II: reliability results and design recoomendations, J. Construct. Steel Res. Comp. Pap. (2016) (Submitted to).
[2] R.D. Ziemian, Advanced Methods of Inelastic Analysis in the Limit States Design of Steel Structures (PhD thesis) Cornell University, Ithaca, NY, 1990.
[3] S.G. Buonopane, B.W. Shafer, Reliability of steel frames designed with advanced analysis, J. Struct. Eng. ASCE 132 (2006) 267–276.
[4] S. Hendawi, D.M. Frangopol, Reliability-based structural system assessment, design and optimization system reliability and redundancy in structural design and evaluation, Struct. Saf. 16 (1994) 47–71.
[5] G. Fu, D.M. Frangopol, Balancing weight, system reliability and redundancy in a multiobjective optimization framework, Struct. Saf. 7 (1990) 165–175.
[6] B.R. Ellingwood, Probability-based codified design: past accomplishments and future challenges, Struct. Saf. 13 (1994) 159–176.
[7] Q. Li, B.R. Ellingwood, Damage inspection and vulnerability analysis of existing buildings with steel moment-resisting frame, Eng. Struct. 30 (2008) 338–351.
[8] H. Zhang, B.R. Ellingwood, K.J.R. Rasmussen, System reliabilities in steel structural frame design by inelastic analysis, Eng. Struct. 81 (2014) 341–348.
[9] A.H. Zubydan, Inelastic second order analysis of steel frame elements flexed about minor axis, Eng. Struct. 33 (2011) 1240–1250.
[10] D.W. White, J.F. Hajjar, Stability of steel frames: the cases for simple elastic and rigorous inelastic analysis/design procedures, Eng. Struct. 22 (2000) 155–167.
[11] N.S. Trahair, S.L. Chan, Out-of-plane advanced analysis of steel structures, Eng. Struct. 25 (2003) 1627–1637.
[12] C. Ngo-Huu, S.E. Kim, J.R. Oh, Nonlinear analysis of space steel frames using fiber plastic hinge concept, Eng. Struct. 29 (2007) 649–657.
[13] H.V. Long, N.D. Hung, Local buckling check according to eurocode-3 for plastichinge analysis of 3-d steel frames, Eng. Struct. 30 (2008) 3105–3113.
[14] S.E. Kim, M.H. Park, S.H. Choi, Direct design of three-dimensional frames using practical advanced analysis, Eng. Struct. 23 (2001) 1491–1502.
[15] M.J. Clarke, R.Q. Bridge, G.J. Hancock, N.S. Trahair, Advanced analysis of steel building frames, J. Constr. Steel Res. 23 (1992) 1–29.
[16] P. Avery, M. Mahendran, Distributed plasticity analysis of steel frame structures comprising non-compact sections, Eng. Struct. 22 (2000) 901–919.
[17] H. Zhang, K.J.R. Rasmussen, System-based design for steel scaffold structures using advanced analysis, J. Constr. Steel Res. 89 (2013) 1–8.
[18] AS4100., Australian Standard AS4100-Steel Structures, Standards Australia., Sydney, NSW 2001, Australia, 2001.
[19] AISC360-10. Specification for Structural Steel Buildings. American Institute of Steel Construction (AISC). Chicago. 2010.
[20] R.D. Ziemian, W. McGuire, G.G. Deierlein, Inelastic limit states design. Part I: planar frame studies, J. Struct. Eng. 118 (1991) 2532–2549.
[21] R.E. Melchers, Structural Reliability Analysis and Prediction, John Wiley & Sons, West Sussex, England, 1999.
[22] ASCE, Minimum Design Loads for Buildings and Other Structures. USA: ASCE Standard 7–05, American Society of Civil Engineers, New York, NY, 2005.
[23] T.V. Galambos, M.K. Ravindar, Properties of steel for use in LRFD, J. Struct. Div. ASCE 104 (1978) 1459–1468.
[24] F.M. Bartlett, R.J. Dexter, M.D. Graeser, J.J. Jelinek, B.J. Schmidt, T.V. Galambos, Updating standard shape material properties database for design and reliability, Eng. J. AISC 40 (2003) 2–14.
[25] J. Melcher, Z. Kala, M. Holický, M. Fajkus, L. Rozlívka, Design characteristics of structural steels based on statistical analysis of metallurgical products, J. Constr. Steel Res. 60 (2004) 795–808.
[26] J. Strating, H. Vos, Computer simulation of the ECCS buckling curve using a Monte-Carlo method, HERON. 19 (1973).
[27] Y. Fukumoto, Y. Itoh, Evaluation of multiple column curves using the experimental data-base approach, J. Constr. Steel Res. 3 (1983) 2–19.
[28] S. Shayan, K.J.R. Rasmussen, H. Zhang, On the modeling of initial geometric imperfections of steel structural frames in advanced analysis, J. Constr. Steel Res. 98 (2014) 167–177.
[29] D. Sfintesco, Fondement experimental des courbes Europeennes de flambement, J. Constr. Métallique. 5–12 (1970).
[30] S. Shayan, K.J.R. Rasmussen, H. Zhang, Probabilistic modelling of residual stress in advanced analysis of steel structures, J. Constr. Steel Res. 101 (2014) 407–414.
[31] B.R. Ellingwood, J.G. Macgregor, T.V. Galambos, C.A. Cornell, Probability based load criteria - load factors and load combinations, J. Struct. Div. ASCE 108 (1982) 978–997.
[32] S. Shayan, System Reliability-Based Design of 2D Steel Frames by Advanced Analysis(PhD thesis) The University of Sydney, Sydney, Australia, 2014.
[33] S. Mazzoni, F. McKenna, M.H. Scott, G.L. Fenves, et al., in: C. PEER (Ed.), OpenSees Command Language Manual, Univ. California at Berkely, Berkely, CA, 2007.
[34] T.V. Galambos, B.R. Ellingwood, J.G. MacGregor, C.A. Cornell, Probability based load criteria: assessment of current design practice, J. Struct. Div. ASCE 108 (1982) 959–977.